SUPPLEMENTAL INFORMATION

Supplemental Experimental Procedures

Fly stocks

The following fly stocks were used: *GluRIIA*^{SP16} (Petersen et al., 1997), *UAS-tor* (Hennig and Neufeld, 2002), *dysbindin*^{1} (Dickman and Davis, 2009), *tor*$^{\Delta P}$ (Penney et al., 2012), *MHC-Gal4* (Schuster et al., 1996), *G14-Gal4* (Aberle et al., 2002), and SynapGCaMP6f (*MHC-CD8-GCaMP6f-Sh*; (Newman et al., 2017)). All other *Drosophila* stocks were obtained from the Bloomington Drosophila Stock Center.

Imaging and analysis: Samples were imaged using a Nikon A1R Resonant Scanning Confocal microscope equipped with NIS Elements software and a 100x APO 1.4NA oil immersion objective using separate channels with four laser lines (405 nm, 488 nm, 561 nm, and 637 nm) as described (Perry et al., 2017). For fluorescence quantifications of BRP and pCamKII intensity levels, z-stacks were obtained using identical settings for all genotypes with z-axis spacing between 0.15 µm to 0.2 µm within an experiment and optimized for detection without saturation of the signal. Maximum intensity projections were used for quantitative image analysis in the NIS Elements software using the general analysis toolkit. Type 1b boutons were counted using vGlut and HRP-stained NMJ terminals on muscle 4 of segment A2, considering each vGlut puncta to be a bouton (Perry et al., 2017). Synapse surface area was calculated by creating a mask around the HRP channel that labels the neuronal membrane. BRP puncta number, area, and mean and sum intensity (average or total sum intensity of individual BRP puncta) were quantified by applying intensity thresholds and filters to binary layers on the BRP labeled 488 channel. For analysis of total integrated pCamKII levels per NMJ, 1b and 1s regions were identified using DLG and HRP on muscle 6/7 and 4 of segment A2 and only the pCamKII pixels that co-localized with DLG and HRP were summated to get total pCamKII intensity levels for an NMJ. Measurements based on confocal images were taken from at least twelve synapses acquired from at least six different animals.

Calcium imaging and analysis

Third-instar larvae were dissected and incubated in ice-cold HL-3 containing a range of Ca^{2+} concentrations (0 mM, 1.5 mM, 5 mM, 10 mM). GCaMP signals were measured at Type-1b boutons on muscle 6/7 of abdominal segments

A2 and A3. The larval central nervous system was removed, and boutons were identified by observing the basal GCaMP fluorescence level in the postsynaptic density as described (Newman et al., 2017). Live imaging was performed using a Nikon A1R Resonant Scanning Confocal microscope equipped with NIS Elements software. Band scanning at a resonant frequency of 113 fps (512 x 86 pixels) was performed across the field of view. Four to eight individual boutons were imaged during each session, lasting for one min. Measurements based on calcium imaging were taken from at least two different animals (approximately 10-12 boutons). Fluorescence events were detected using regions of interest (ROIs) that were manually drawn around individual boutons. ΔF was calculated by subtracting the basal GCaMP fluorescence level from the peak intensity of the GCaMP signal at a particular bouton. ΔF was then divided by the average fluorescence value of a reference ROI, which had no detectible events, to obtain the ΔF/F value. The total time over which the GCaMP signal was above basal levels was used to determine decay time.

Immunocytochemistry: Third-instar larvae were dissected in ice cold 0 Ca^{2+} HL-3 and immunostained as described (Kikuma et al., 2017). The following antibodies were used: mouse anti-Bruchpilot (BRP; nc82; 1:100; Developmental Studies Hybridoma Bank; DSHB); rabbit anti-DLG (1:100; (Pielage et al., 2005); guinea pig anti-vGlut (1:2000; (Chen et al., 2017)), mouse anti-pCamKII (MA1-047; 1:100; Invitrogen). Donkey anti-mouse, anti-guinea pig, and anti-rabbit Alexa Fluor 488- and Cyanine 3 (Cy3)-conjugated secondary antibodies (Jackson Immunoresearch) were used at 1:400. Alexa Fluor 647 conjugated goat anti-HRP (Jackson ImmunoResearch) was used at 1:200.

Electrophysiology

All dissections and recordings were performed in modified HL3 saline (Dickman et al., 2005; Kiragasi et al., 2017; Stewart et al., 1994) containing (in mM): 70 NaCl, 5 KCl, 10 $MgCl_2$, 10 $NaHCO_3$, 115 Sucrose, 5 Trehelose, 5 HEPES, pH 7.2 and supplemented with different concentrations of $CaCl_2$ (0 mM, 0.3, 1.5 mM, 5 mM and 10 mM, as specified). Neuromuscular junction sharp electrode (electrode resistance between 10-35 MΩ) recordings were performed on muscles 6 and 7 of abdominal segments A2 and A3 in wandering third-instar larvae. Larvae were dissected and loosely pinned; the guts, trachea, and ventral nerve cord were removed from the larval body walls with the motor nerve cut, and the preparation was perfused several times with HL3 saline. Recordings were performed on

an Olympus BX61 WI microscope using a 40x/0.80 water-dipping objective, and acquired using an Axoclamp 900A amplifier, Digidata 1440A acquisition system and pClamp 10.5 software (Molecular Devices). Electrophysiological sweeps were digitized at 10 kHz and filtered at 1 kHz. Data were analyzed using Clampfit (Molecular devices), MiniAnalysis (Synaptosoft), Excel (Microsoft), and SigmaPlot (Systat) software. Miniature excitatory postsynaptic potentials (mEPSPs) were recorded in the absence of any stimulation. Muscle input resistance (R_{in}) and resting membrane potential (V_{rest}) were monitored during each experiment. Recordings were rejected if the V_{rest} was above -60 mV, if the R_{in} was less than 5 MΩ, or if either measurement deviated by more than 10% during the course of the experiment. An ISO-Flex stimulus isolator (A.M.P.I.) was used to modulate the amplitude of stimulatory currents. Intensity was adjusted for each cell, set to consistently elicit responses from both neurons innervating the muscle segment, but avoiding overstimulation. Average mEPSP, EPSP, and quantal content were calculated for each genotype with or without corrections for nonlinear summation (Martin, 1955).

Statistical Analysis

Data were compared using either a one-way ANOVA followed by Tukey's multiple comparison test, or using a Student's t-test (where specified), analyzed using Graphpad Prism or Microsoft Excel software.

Supplemental References

Aberle, H., Haghighi, A.P., Fetter, R.D., McCabe, B.D., Magalhaes, T.R., and Goodman, C.S. (2002). wishful thinking encodes a BMP type II receptor that regulates synaptic growth in Drosophila. Neuron *33*, 545-558.

Chen, X., Ma, W., Zhang, S., Paluch, J., Guo, W., and Dickman, D.K. (2017). The BLOC-1 Subunit Pallidin Facilitates Activity-Dependent Synaptic Vesicle Recycling. eNeuro *4*, 1-18.

Dickman, D.K., and Davis, G.W. (2009). The schizophrenia susceptibility gene dysbindin controls synaptic homeostasis. Science 326, 1127-1130.

Dickman, D.K., Horne, J.A., Meinertzhagen, I.A., and Schwarz, T.L. (2005). A slowed classical pathway rather than kiss-and-run mediates endocytosis at synapses lacking synaptojanin and endophilin. Cell 123, 521-533.

Hennig, K.M., and Neufeld, T.P. (2002). Inhibition of cellular growth and proliferation by dTOR overexpression in Drosophila. Genesis, 107-110.

Kikuma, K., Li, X., Kim, D., Sutter, D., and Dickman, D.K. (2017). Extended Synaptotagmin Localizes to Presynaptic ER and Promotes Neurotransmission and Synaptic Growth in Drosophila. Genetics.

Kiragasi, B., Wondolowski, J., Li, Y., and Dickman, D.K. (2017). A Presynaptic Glutamate Receptor Subunit Confers Robustness to Neurotransmission and Homeostatic Potentiation. Cell Rep 19, 2694-2706.

Martin, A.R. (1955). A further study of the statistical composition on the end-plate potential. J Physiol 130, 114-122.

Newman, Z.L., Hoagland, A., Aghi, K., Worden, K., Levy, S.L., Son, J.H., Lee, L.P., and Isacoff, E.Y. (2017). Input-Specific Plasticity and Homeostasis at the Drosophila Larval Neuromuscular Junction. Neuron 93, 1388-1404.

Penney, J., Tsurudome, K., Liao, E.H., Elazzouzi, F., Livingstone, M., Gonzalez, M., Sonenberg, N., and Haghighi, A.P. (2012). TOR is required for the retrograde regulation of synaptic homeostasis at the Drosophila neuromuscular junction. Neuron 74, 166-178.

Perry, S., Han, Y., Das, A., and Dickman, D.K. (2017). Homeostatic plasticity can be induced and expressed to restore synaptic strength at neuromuscular junctions undergoing ALS-related degeneration. Human Mol Genet.

Petersen, S.A., Fetter, R.D., Noordermeer, J.N., Goodman, C.S., and DiAntonio, A. (1997). Genetic analysis of glutamate receptors in Drosophila reveals a retrograde signal regulating presynaptic transmitter release. Neuron 19, 1237-1248.

Pielage, J., Fetter, R.D., and Davis, G.W. (2005). Presynaptic Spectrin Is Essential for Synapse Stabilization. Curr Biol 15, 918-928.

Schuster, C.M., Davis, G.W., Fetter, R.D., and Goodman, C.S. (1996). Genetic Dissection of Structural and Functional Components of Synaptic Plasticity. II. Fasciclin II Controls Presynaptic Structural Plasticity. Neuron 17, 655-667.

Stewart, B.A., Atwood, H.L., Renmger, J.J., Wang, J., and Wu, C.F. (1994). Improved stability of Drosophila larval neuromuscular prepa- rations in haemolymph-like physiological solutions. J Comp Physiol 175, 179-191.

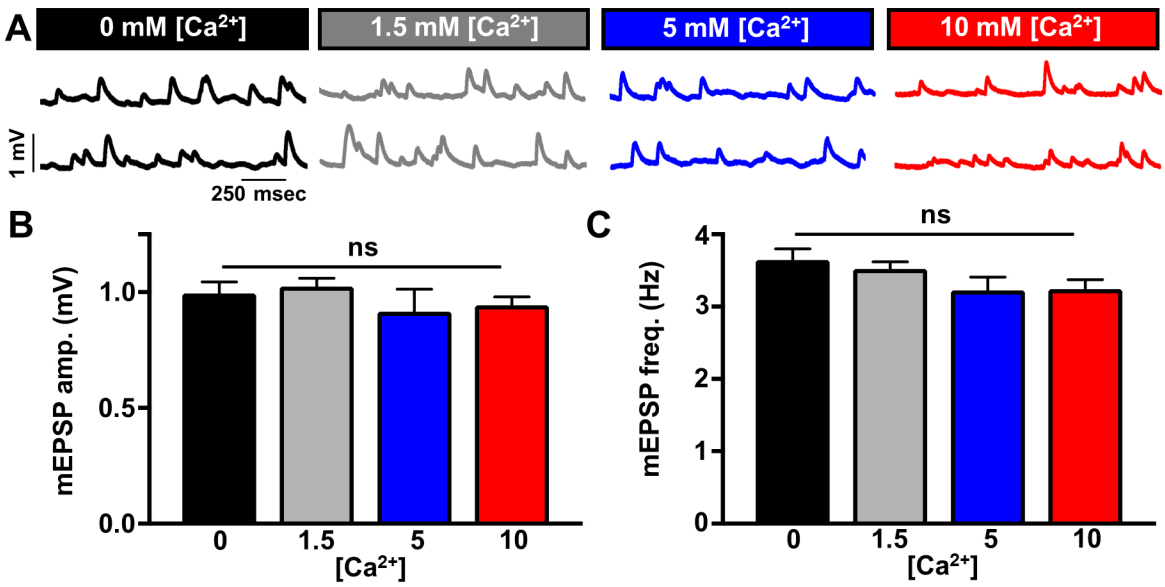
A
0 mM [Ca2+]
1.5 mM [Ca2+]
5 mM [Ca2+]
10 mM [Ca2+]
1 mV
250 msec
B
mEPSP amp. (mV)
ns
1.0
0.5
0.0
0
1.5
5
10
[Ca2+]
C
mEPSP freq. (Hz)
ns
4
3
2
1
0
0
1.5
5
10
[Ca2+]

Supplemental Figure S1: mEPSP amplitude and frequency are not significantly changed across a range of extracellular Ca^{2+} concentrations at the *Drosophila* NMJ, related to Figure 4. (A) Representative traces of mEPSP recordings at wild-type NMJs in four different extracellular calcium concentrations are shown. Quantification of mEPSP amplitude **(B)** and mEPSP frequency **(C)** demonstrates that these parameters are not significantly affected by extracellular Ca^{2+} concentrations. Error bars indicate ±SEM. One-way analysis of variance (ANOVA) test was performed, followed by a Tukey's multiple-comparison test. ns=not significant, $p>0.05$. Detailed statistical information (mean values, SEM, n, p) is shown in Table S1

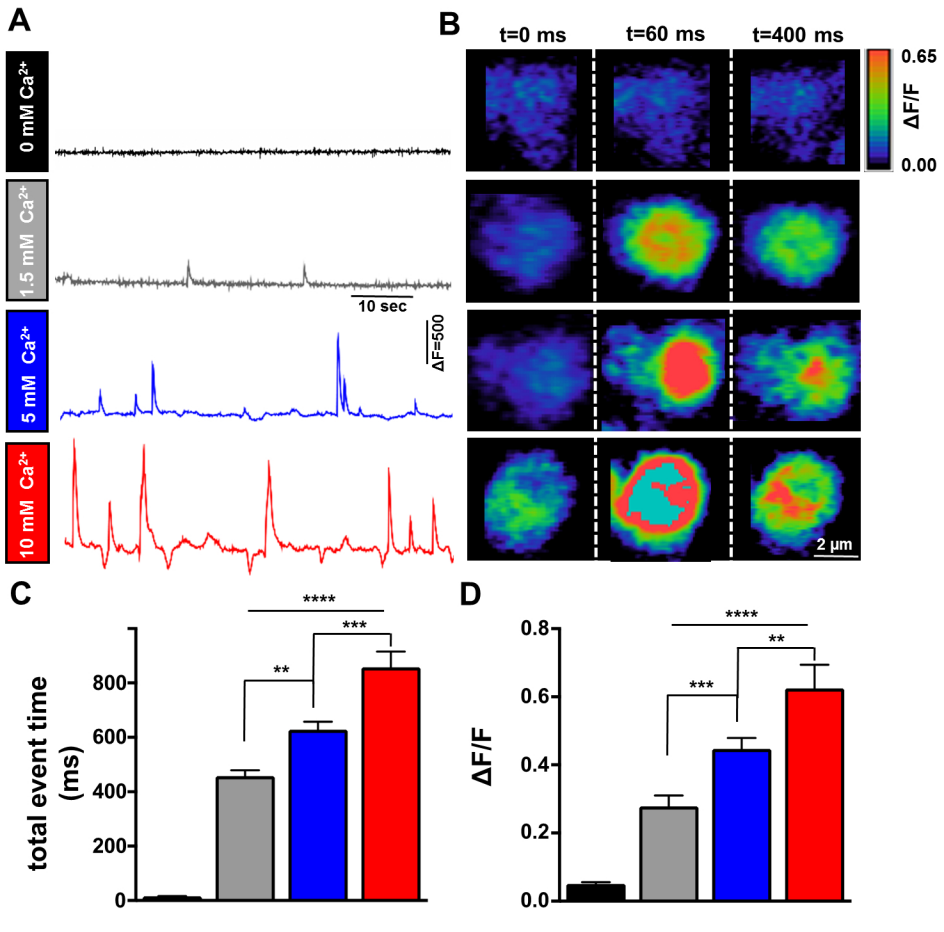
A
0 mM Ca2+
1.5 mM Ca2+
5 mM Ca2+
10 mM Ca2+
10 sec
ΔF=500
B
t=0 ms
t=60 ms
t=400 ms
0.65
ΔF/F
0.00
2 μm
C
total event time (ms)
0
200
400
600
800
**
***
****
D
ΔF/F
0.0
0.2
0.4
0.6
0.8
***
**
****

Supplemental Figure S2: Postsynaptic Ca^{2+} transients are enhanced with increasing extracellular Ca^{2+} concentrations, related to Figure 4. (A) Representative images of Ca^{2+} transients during spontaneous mEPSP events at the *Drosophila* NMJ. While no transients are observed in 0 mM Ca^{2+}, increasing extracellular Ca^{2+} leads to correlated enhancements in the observed Ca^{2+} signal, imaged using SynapGCaMP6F (Newman et al., 2017). **(B)** Representative images of GCaMP signals at individual boutons shown at three different time points (0, 40, and 600 msec). The Ca^{2+} signal peaks at ~60 msec, and the magnitude of the peak correlates with the extracellular Ca^{2+} concentration. Quantification of the total event time **(C)** and ΔF/F signals **(D)**. The peak fluorescence signal was normalized to the average SynapGCaMP6F signal (at baseline) for the bouton being considered to obtain ΔF/F. Error bars indicate ±SEM. One-way analysis of variance (ANOVA) test was performed, followed by a Tukey's multiple-comparison test. **p≤0.01; ***p≤0.001; ****p≤0.0001; ns=not significant, p>0.05. Detailed statistical information (mean values, SEM, n, p) is shown in Table S1.

Table 1: Absolute values for normalized data and additional statistics, related to Figures 1-4, S1 and S2. The figure and panel, genotype, and conditions used are noted (external calcium concentration and whether PhTx was applied). For electrophysiological recordings, average values for mEPSP, EPSP, quantal content (QC), resting potential, input resistance, number of data samples (n), p values, and significance are shown. For confocal imaging analysis, average values for intensity levels of different synaptic markers are shown. Standard error values are noted in parentheses. Rows highlighted in blue are the respective controls/baseline values for the particular experiment being referenced.

Figure	Genotype	$[Ca^{2+}]$	PhTx	mEPSP (mV)	EPSP (mV)	QC	Resting Potential (mV)	Input Resistance (MΩ)	n	P value (significance) (mEPSP, EPSP, QC)
1B,C,D	w^{1118}	0.3	-	0.977 (0.024)	22.720 (0.656)	23.470 (0.965)	-64.501 (0.940)	9.221 (0.987)	17	
1B,C,D	w^{1118}	0.3	+	0.505 (0.012)	21.560 (0.610)	42.910 (1.406)	-69.269 (1.466)	8.932 (0.802)	14	<0.0001 (****), 0.8797 (ns), <0.0001 (****)
1B,C,D	w^{1118}; $GluRIIA^{sp16}$	0.3	-	0.486 (0.027)	19.76 (0.981)	41.400 (2.931)	-69.292 (2.473)	10.199 (0.972)	8	<0.0001 (****), 0.1861 (ns), <0.0001 (****)
1B,C,D	w^{1118}; MHC-Gal4/UAS-Tor	0.3	-	0.999 (0.040)	34.590 (0.967)	35.020 (1.130)	-66.451 (1.830)	12.433 (1.181)	13	0.9913 (ns), <0.0001 (****), <0.0001 (****)
1B,C,D	w^{1118}; $GluRIIA^{sp16}$; MHC-Gal4/UAS-Tor	0.3	-	0.476 (0.022)	16.580 (0.791)	38.050 (2.224)	-62.166 (1.252)	11.989 (1.299)	8	<0.0001 (****), <0.0001 (****), 0.8505 (ns)
1B,C,D	w^{1118}; MHC-Gal4/UAS-Tor	0.3	+	0.576 (0.013)	21.590 (1.559)	37.820 (3.317)	-67.578 (2.518)	10.996 (0.913)	7	<0.0001 (****), <0.0001 (****), 0.9039 (ns)
Figure	**Genotype**	**$[Ca^{2+}]$**	**PhTx**	**mEPSP (mV)**	**EPSP (mV)**	**QC**	**Resting Potential (mV)**	**Input Resistance (MΩ)**	**n**	**P value (significance) (mEPSP, EPSP, QC)**
3B,C,D	w^{1118}	0.3	+	0.505 (0.012)	21.560 (0.610)	42.910 (1.406)	-69.269 (1.466)	8.932 (0.802)	14	<0.0001 (****), 0.8797 (ns), <0.0001 (****) (baseline:Fig1 WT)
3B,C,D	w^{1118};$dysb^{1}$	0.3	-	0.901 (0.045)	24.990 (1.529)	27.970 (1.603)	-70.156 (1.541)	7.977 (0.655)	11	
3B,C,D	w^{1118};$dysb^{1}$	0.3	+	0.534 (0.042)	11.290 (0.545)	21.770 (1.337)	-68.311 (1.698)	9.222 (0.820)	9	<0.0001(****), <0.0001 (****), 0.4691 (ns)
3B,C,D	w^{1118}; $GluRIIA^{sp16}$;$dysb^{1}$	0.3	-	0.449 (0.026)	9.852 (1.006)	23.310 (3.003)	-61.211 (1.272)	10.390 (1.209)	18	<0.0001 (****), <0.0001 (****), 0.5574 (ns)
3B,C,D	w^{1118}; G14-Gal4/UAS-Tor; $dysb^{1}$	0.3	-	0.935 (0.035)	21.150 (1.623)	23.530 (3.545)	-68.231 (1.599)	12.506 (1.771)	13	0.9283 (ns), 0.1913 (ns), 0.6615 (ns),

Figure	Genotype	$[Ca^{2+}]$	PhTx	CHX	mEPSP (mV)	EPSP (mV)	QC	Resting Potential (mV)	Input Resistance (MΩ)	n	P value (significance) (mEPSP, EPSP, QC)
4B	w^{1118}	0.3	+	-	0.515 (0.013)	22.030 (0.910)	43.120 (2.394)	-70.381 (2.106)	8.932 (0.802)	9	<0.0001 (****), 0.8797 (ns), <0.0001 (****) (baseline:Fig1 WT)
4B	w^{1118}	0.3	+	+	0.479 (0.021)	19.300 (0.623)	41.520 (2.778)	-62.782 (3.141)	8.224 (0.735)	12	0.8787 (ns), 0.2409 (ns), 0.9717 (ns)
1B,C,D	w^{1118}; $GluRIIA^{SP16}$	0.3	-	-	0.486 (0.027)	19.76 (0.981)	41.400 (2.931)	-69.292 (2.473)	10.199 (0.972)	8	<0.0001 (****), 0.1861 (ns), <0.0001 (****) (baseline:Fig1 WT)
4B	w^{1118}; $GluRIIA^{sp16}$	0.3	-	+	0.436 (0.014)	15.060 (0.959)	34.800 (2.250)	-65.315 (1.529)	9.003 (0.851)	13	0.8295 (ns), 0.0135 (*) 0.3997 (ns)
1B,C,D	w^{1118}; MHC-Gal4/UAS-Tor	0.3	-	-	0.999 (0.040)	34.590 (0.967)	35.020 (1.130)	-66.451 (1.830)	12.433 (1.181)	13	0.9913 (ns), <0.0001 (****), <0.0001 (****) (baseline:Fig1 WT)
4B	w^{1118}; MHC-Gal4/UAS-Tor	0.3	-	+	0.949 (0.071)	30.440 (1.463)	33.260 (2.498)	-61.297 (1.352)	12.592 (0.987)	9	0.9076 (ns), 0.0492 (*), 0.8505 (ns)

Figure	Genotype	[Ca^{2+}]	PhTx	mEPSP (mV)	EPSP (mV)	QC	Resting Potential (mV)	Input Resistance (MΩ)	n	P value (significance) (mEPSP, EPSP, QC)
4C	w^{1118}	0.3	-	1.028 (0.04)	22.000 (1.52)	21.890 (2.17)	-67.996 (1.56)	7.583 (0.513)	8	
4C	w^{1118}; $tor^{\Delta P}$/+	0.3	-	1.058 (0.04)	25.490 (2.17)	24.280 (2.06)	-65.33 (1.72)	9.273 (0.768)	7	0.9379 (ns), <0.3680 (ns), 0.9176 (ns)
4C	w^{1118}; $GluRIIA^{sp16}$, $tor^{\Delta P}$/ $GluRIIA^{sp16}$	0.3	-	0.449 (0.02)	10.860 (0.88)	24.640 (2.35)	-64.86 (2.33)	10.361 (1.085)	8	<0.0001 (****), <0.0001 (****), 0.8695 (ns)
4C	w^{1118}; $tor^{\Delta P}$/+	0.3	+	0.517 (0.03)	21.460 (1.19)	42.870 (3.75)	-61.67 (1.18)	8.909 (0.874)	7	<0.0001 (****), 0.9940 (ns), <0.0001 (****)
Figure	**Genotype**	**[Ca^{2+}]**	**Incubation conditions**	**mEPSP (mV)**	**EPSP (mV)**	**QC**	**Resting Potential (mV)**	**Input Resistance (MΩ)**	**n**	**P value (significance) (mEPSP, EPSP, QC)**
4H	w^{1118}	0.4	(1.5 Ca^{2+})	1.192 (0.044)	33.388 (1.273)	28.010 (1.976)	-67.912 (1.176)	9.065 (0.711)	7	
4H	w^{1118}	0.4	(0 Ca^{2+}) +PhTx	0.500 (0.020)	30.410 (1.751)	61.870 (4.636)	-68.653 (0.865)	7.902 (0.659)	10	<0.0001 (****), 0.7026 (ns), 0.0031 (***)
4H	w^{1118}	0.4	(0.0 Ca^{2+})	1.187 (0.028)	36.857 (1.273)	33.740 (2.008)	-70.832 (2.113)	8.036 (0.671)	8	0.8967 (ns), 0.9887 (ns), 0.8944 (ns)

Figure	Genotype	[Ca^{2+}] (mM)	mEPSP amplitude (mV)	mEPSP frequency (Hz)	n	P value (significance) (mEPSP amplitude, mEPSP frequency)
S1B, C	w^{1118}	0	0.943 (0.036)	3.644 (0.155)	6	
S1B, C	w^{1118}	1.5	0.916 (0.117)	3.226 (0.182)	7	0.9931 (ns), 0.2113 (ns)
S1B, C	w^{1118}	5	1.024 (0.036)	3.242 (0.130)	7	0.8622 (ns), 0.2381 (ns)
S1B, C	w^{1118}	10	0.994 (0.049)	3.521 (0.098)	6	0.9654 (ns), 0.9218 (ns)

Figure	Genotype	PhTx	Bouton #/NMJ	BRP #/NMJ	BRP density (#/ μm^2)	BRP puncta area (μm^2)	n	P value (significance) (Bouton #, BRP #, density, area)
2B,C,D,E	w^{1118}	-	28.610 (1.500)	213.400 (7.358)	1.315 (0.056)	0.154 (0.005)	24	
2B,C,D,E	w^{1118}	+	23.160 (1.264)	208.800 (10.750)	1.208 (0.055)	0.221 (0.010)	18	0.3173 (ns), 0.9993 (ns), 0.7414 (ns), <0.0001 (****)
2B,C,D,E	w^{1118}; $GluRIIA^{sp16}$	-	23.640 (1.977)	202.500 (23.130)	1.268 (0.103)	0.211 (0.014)	14	0.2781 (ns), 0.9849 (ns), 0.9910 (ns), 0.0003 (***)
	w^{1118}; $dysb^{1}$	-	23.775 (1.273)	210.333 (4.998)	1.361 (0.087)	0.170 (0.011)	17	0.4791 (ns), 0.8428 (ns), 0.4003 (ns), 0.6798 (ns)
2B,C,D,E	w^{1118}; *MHC-Gal4/UAS-Tor*	-	23.630 (2.569)	206.000 (17.650)	1.227 (0.065)	0.208 (0.039)	17	0.9242 (ns), 0.9953 (ns), 0.8725 (ns), 0.0001 (***)
2B,C,D,E	w^{1118}; *MHC-Gal4/UAS-Tor*	+	26.530 (1.609)	226.600 (13.230)	1.301 (0.102)	0.205 (0.014)	11	0.7994 (ns), 0.8441 (ns), 0.9627 (ns), 0.9986 (ns)

Figure	Genotype	PhTx	BRP puncta mean intensity (%WT)	BRP puncta sum intensity (%WT)	n	P value (significance) (BRP puncta mean intensity, BRP puncta sum intensity)
2B,C,D,E	w^{1118}	-	100.000 (6.172)	100.000 (8.566)	24	
2B,C,D,E	w^{1118}	+	126.553 (7.865)	160.587 (10.371)	18	0.0071 (**), <0.0001 (****)
2B,C,D,E	w^{1118}; $GluRIIA^{sp16}$	-	127.777 (5.243)	168.273 (11.871)	14	0.0029 (**),<0.0001 (****)
	w^{1118}; $dysb^{1}$	-	111.709 (4.222)	100.790 (6.681)	17	0.6781 (ns), 0.9498 (ns)
2B,C,D,E	w^{1118}; *MHC-Gal4/UAS-Tor*	-	125.908 (5.708)	190.170 (8.795)	17	0.0014 (**),<0.0001 (****)
2B,C,D,E	w^{1118}; *MHC-Gal4/UAS-Tor*	+	120.004 (8.797)	185.494 (7.136)	11	>0.9999 (ns), 0.9980 (ns)

2B,C,D,E	w^{1118}; *MHC-Gal4/UAS-Tor*	-	23.630 (2.569)	206.000 (17.650)	1.227 (0.065)	0.208 (0.039)	17	0.9242 (ns), 0.9953 (ns), 0.8725 (ns), 0.0001 (***)
2B,C,D,E	w^{1118}; *MHC-Gal4/UAS-Tor*	+	26.530 (1.609)	226.600 (13.230)	1.301 (0.102)	0.205 (0.014)	11	0.7994 (ns), 0.8441 (ns), 0.9627 (ns), 0.9986 (ns)

Figure	Genotype	PhTx	BRP puncta mean intensity (%WT)	BRP puncta sum intensity (%WT)	n	P value (significance) (BRP puncta mean intensity, BRP puncta sum intensity)
2B,C,D,E	w^{1118}	-	100.000 (6.172)	100.000 (8.566)	24	
2B,C,D,E	w^{1118}	+	126.553 (7.865)	160.587 (10.371)	18	0.0071 (**), <0.0001 (****)
2B,C,D,E	w^{1118}; $GluRIIA^{sp16}$	-	127.777 (5.243)	168.273 (11.871)	14	0.0029 (**),<0.0001 (****)
	w^{1118}; $dysb^{1}$	-	111.709 (4.222)	100.790 (6.681)	17	0.6781 (ns), 0.9498 (ns)
2B,C,D,E	w^{1118}; MHC-Gal4/UAS-Tor	-	125.908 (5.708)	190.170 (8.795)	17	0.0014 (**),<0.0001 (****)
2B,C,D,E	w^{1118}; MHC-Gal4/UAS-Tor	+	120.004 (8.797)	185.494 (7.136)	11	>0.9999 (ns), 0.9980 (ns)

Figure	Genotype	PhTx	Extracellular [Ca^{2+}]	Total CamKII intensity (%WT)	n	P value (significance)
2B,C,D,E	w^{1118}	-	0.4 mM	100 (8.265)	11	
2B,C,D,E	w^{1118}	+	0.4 mM	61.813 (5.112)	13	0.0039 (**)
2B,C,D,E	w^{1118}; $GluRIIA^{sp16}$	-	0.4 mM	61.621 (6.102)	13	0.0012 (**)
2B,C,D,E	w^{1118}; MHC-Gal4/UAS-Tor	-	0.4 mM	128.835 (0.119)	15	0.0817 (ns)

Figure	Genotype	PhTx	Extracellular [Ca^{2+}]	Total CamKII intensity (%WT)	n	P value (significance)
2B,C,D,E	w^{1118}	-	0.4 mM	100.632 (8.724)	11	
2B,C,D,E	w^{1118}	-	0.0 mM	100.000 (7.812)	19	0.9592 (ns)
2B,C,D,E	w^{1118}	+	0.4 mM	62.856 (4.796)	13	0.0029 (**)
2B,C,D,E	w^{1118}	+	0 .0 mM	55.151 (4.399)	11	0.0012 (**)

Figure	Genotype	[Ca^{2+}] (mM)	Total Event Time (ms)	ΔF/F (a.u.)	n	P value (significance) (total event time, ΔF/F)
S2C, D	w^{1118}	0	15.46 (0.559)	0.03 (0.002)	8	<0.0001 (****), <0.0001 (****)
S2C, D	w^{1118}	1.5	457.80 (21.160)	0.27 (0.032)	12	
S2C, D	w^{1118}	5	627.40 (29.64)	0.45 (0.032)	11	0.005 (**), 0.0004 (***)
S2C, D	w^{1118}	10	857.80 (57.85)	0.63 (0.071)	10	0.0002 (***), <0.0001 (****)